Optical trapping of nanotubes with cylindrical vector beams

M. G. Donato,[1,*] S. Vasi,[1] R. Sayed,[1,2] P. H. Jones,[3] F. Bonaccorso,[4] A. C. Ferrari,[4] P. G. Gucciardi,[1] and O. M. Maragò[1]

[1]CNR-IPCF, Istituto per i Processi Chimico-Fisici, V.le F. Stagno d'Alcontres 37, 98158 Messina, Italy

[2]Universitá di Messina, V.le F. Stagno d'Alcontres 31, 98166 S. Agata-Messina, Italy

[3]Department of Physics and Astronomy, University College London, WC1E 6BT London, UK

[4]Engineering Department, University of Cambridge, 9 JJ Thomson Ave., Cambridge CB3 0FA, UK

*Corresponding author: donato@me.cnr.it

Received June 12, 2012; revised July 4, 2012; accepted July 4, 2012;
posted July 5, 2012 (Doc. ID 170435); published August 8, 2012

We use laser beams with radial and azimuthal polarization to optically trap carbon nanotubes. We measure force constants and trap parameters as a function of power showing improved axial trapping efficiency with respect to linearly polarized beams. The analysis of the thermal fluctuations highlights a significant change in the optical trapping potential when using cylindrical vector beams. This enables the use of polarization states to shape optical traps according to the particle geometry, as well as paving the way to nanoprobe-based photonic force microscopy with increased performance compared to a standard linearly polarized configuration. © 2012 Optical Society of America

OCIS codes: 140.7010, 350.4855.

Optical tweezers [1] (OT) are tools for contactless manipulation of particles [2], as well as transduction and sensing of subpiconewton forces [3]. The great versatility of OT has allowed their application in several research fields, including physics [3] and life sciences [2,4]. However, trapping particles smaller than the wavelength of light is generally difficult [2]. Optical forces scale approximately with size [2]; thus such particles experience reduced trapping forces, being then more prone to the destabilizing effect of thermal fluctuations [4]. As a consequence, the approach to trap nanosized objects is to exploit the enhancement of radiation forces arising either from their intrinsic optical properties, such as plasmon resonances [5,6], or from their highly anisotropic geometry, as for nanotubes [7], graphene [8], nanowires [9–11], and more complex aggregated nanoparticles [12,13].

Enhancement, or even tailoring, of optical forces can be obtained by the careful choice of the trapping beam properties (such as intensity profile and polarization state). Optical trapping takes great benefit from, or has even stimulated [14], advanced studies on shaped or structured light beams [15]. As an example, laser "tractor" beams [16] can be realized by focusing Bessel beams to trap particles with a strong multipolar response to the incoming light field [17]. In this context, the properties of cylindrical vector beams (CVBs) have attracted great interest [14,15]. CVBs are solutions to the vector Helmholtz equation in cylindrical coordinates [15] and, in contrast to the paraxial solutions in Cartesian coordinates (e.g., Hermite–Gauss beams), possess azimuthal symmetry in both amplitude and polarization direction [18,19]. The electric field direction has an inhomogeneous distribution in the laser beam cross section [18,19]. For the lowest order modes, the electric field vector makes a constant angle ϕ_0 with the radius [see Fig. 1(a)]. As the polarization is not defined at the optical axis [18], such beams have a dark center enclosed by a bright ring [19]. Beams having $\phi_0 = 0$ and $\phi_0 = \pi/2$ are radially and azimuthally polarized, respectively [see Figs. 1(b) and 1(c)]. The CVB focusing properties and their application to optical trapping of spherical particles have been recently investigated both theoretically [20–25] and experimentally [26–31]. When focused by a high numerical aperture (NA) objective, azimuthally polarized beams yield a focal spot with a ring-shaped intensity distribution and zero field on axis [24]. This allows low refractive index particles to be trapped [21]. Moreover, radially polarized beams have an on-axis intensity maximum due to a strong longitudinally polarized electric field component [18,24]. Thus, an increased gradient force is expected in the beam propagation (axial) direction, increasing their axial trapping efficiency compared to linear polarized beams [23].

Here we use radially and azimuthally polarized laser beams to trap single-wall carbon nanotube (SWNT) bundles. We measure optical force constants and trap geometry parameters by analyzing their fluctuations, and compare them to those obtained under linear polarization. We compare their dependence with laser power, highlight the significant change in the optical trapping

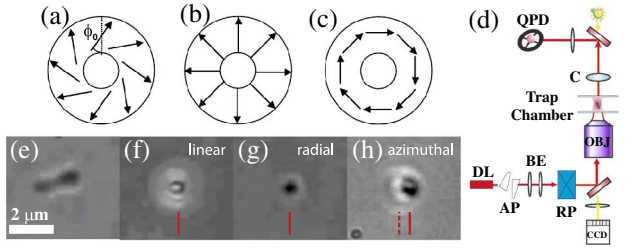

Fig. 1. (Color online) Sketch of (a) generic cylindrical vector, (b) radially and (c) azimuthally polarized beam, and (d) experimental scheme (see text for details). Images of (e) free floating single-wall carbon nanotube (SWNT) bundle, and of a trapped bundle under (f) linear, (g) radial, and (h) azimuthal polarization. The vertical red lines in (f)-(h) show the center of the diffraction limited SWNT bundle image (solid line), which in the case of azimuthal polarization is shifted from the trap center (dashed line).

potential, and show the benefits of CVBs for optical trapping of elongated [one-dimensional (1D)] nanostructures. Thus these unconventional polarization states (radially and azimuthally polarized beams) provide an additional degree of control over the optical potential that can be exploited when using linear nanoprobes in photonic force microscopy applications [7,9,11,12].

Our OT apparatus [see scheme in Fig. 1(d)] is based on a near-infrared (wavelength, $\lambda = 830$ nm) diode laser (DL) and a high NA (1.3) objective (Olympus 100×) [7]. The beam is collimated by an aspheric lens and circularized by a pair of anamorphic prisms (AP). After beam expansion (BE) with a telescope, radial or azimuthal polarization is obtained by means of a commercial liquid-crystal radial polarizer (RP), ARCoptix [31]. The samples are loaded in a small round chamber with volume ~80 μl, and a CCD camera is used to view and record images of the trapped particles via the same objective that is used for trapping [see Figs. 1(e)–1(h)]. Optical force measurements, calibration of the OT, and Brownian motion analysis are performed by collecting the laser light forward scattered by the trapped particle through a condenser lens (C) onto a quadrant photodiode (QPD) and recording the tracking signals of the trapped tubes. Their temporal correlation function analysis yields the spring constants, k_x, k_y, k_z, of the optical trap [7].

We use SWNTs as test 1D nanoparticles since they can be dispersed in liquids through well-established procedures [32] and efficiently trapped [7]. Our samples are produced with the following steps, chosen for their simplicity. We use CoMoCAT nanotube soot (SouthWest NanoTechnologies) dispersed in 0.2% w/v aqueous solution of Taurodeoxycholate, since this is an efficient surfactant to obtain small nanotube bundles [32]. Ultracentrifugation is used for the removal of insoluble materials and residual large bundles. The remaining bundles have a transverse size ~10 nm [7] while their length is in the micrometer range [7]. Note that transverse size has a logarithmic contribution to the bundle hydrodynamics [7], the length being the most relevant parameter [11]. In all our measurements, SWNT bundles ~2 μm long are stably trapped at a distance of ~8 μm from the coverslip surface. Figure 2 shows the measured spring constants as a function of laser power under linear, radial, and azimuthal polarization. The slope, k_i/P, of the linear fit to the experimental data in Fig. 2 is a direct measurement of the trapping efficiencies (see Table 1). We find that the transverse spring constants are stronger (e.g., k_x is a factor ~2 higher) in linear polarization, while the axial spring constant is highest in radial (a factor ~1.2) and azimuthal (a factor ~1.5) polarization. The latter case is unexpected, because for this polarization the z-component of the focused electric field is absent [18], yielding zero intensity on axis. The annular intensity distribution of azimuthal polarization enables stable optical trapping at the focal point only for particles with size larger than the dark region of the focused beam [21]. Instead, for particles smaller than the dark spot, stable trapping occurs on the bright ring as shown in Fig. 1(h) with a spring constant comparable to that of the radial polarization case. Stable trapping at any point around the circumference of the doughnut-shaped focus is

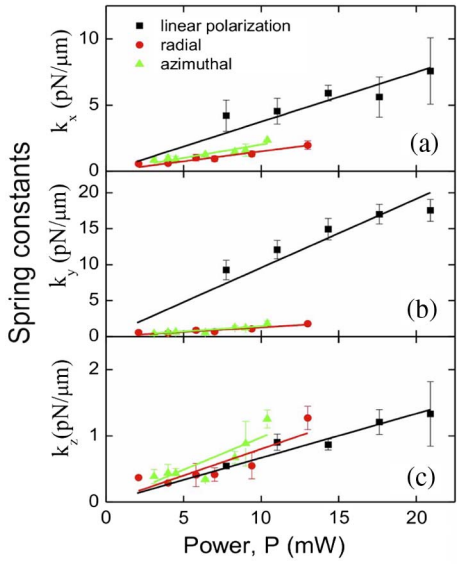

Fig. 2. (Color online) Optical force constants as a function of laser power at the sample for nanotubes trapped under linear (squares), radial (circles), and azimuthal (triangles) polarization. Linear fits to the data are also shown.

expected if the beam maintains its azimuthal symmetry; however, in our experiment, this is not the case due to residual astigmatism in the beam from the laser diode, and differences in the reflection coefficients for s- and p-polarized light of the optics in the microscope. This being the case, we expect a (small) intensity modulation around the circumference of the doughnut focus, and two preferred trapping locations at diametrically opposed points.

The shape of the trapping potential can be studied by means of two parameters, the polarization asymmetry $k_p = 1 - k_x/k_y$ [7] and the trap aspect ratio $k_{\mathrm{ar}} = (k_x + k_y)/2k_z$ [10]. Figure 3 plots k_p, k_{ar} as a function of laser power for the three polarizations. For nanotubes trapped with a linearly polarized beam, we get $k_p = 0.60 \pm 0.05$ and $k_{\mathrm{ar}} = 11 \pm 2$, in good agreement with optical trapping calculations based on T-matrix methods for linear nanostructures [10]. In the case of radial and azimuthal polarization, the expected k_p is zero, due to the cylindrical symmetry of the beams. Our data give $k_p \sim -0.2 \pm 0.2$ and -0.6 ± 0.4, respectively. Residual beam asymmetry (as discussed above) results in this small negative k_p for radial polarization. For azimuthal polarization, the average negative value reflects the trapping on the side of the focal spot. We also note that, at low power, the data are more scattered, reflecting the inherent difficulty in trapping under azimuthal polarization at low power.

Table 1. Trapping Efficiencies under Linear, Radial, and Azimuthal Polarization, with Error Bars in Brackets

(pN/nmW)	Linear	Radial	Azimuthal
k_x/P	0.37(0.03)	0.15(0.01)	0.20(0.01)
k_y/P	0.96(0.05)	0.13(0.01)	0.14(0.01)
k_z/P	0.067(0.003)	0.08(0.01)	0.098(0.009)

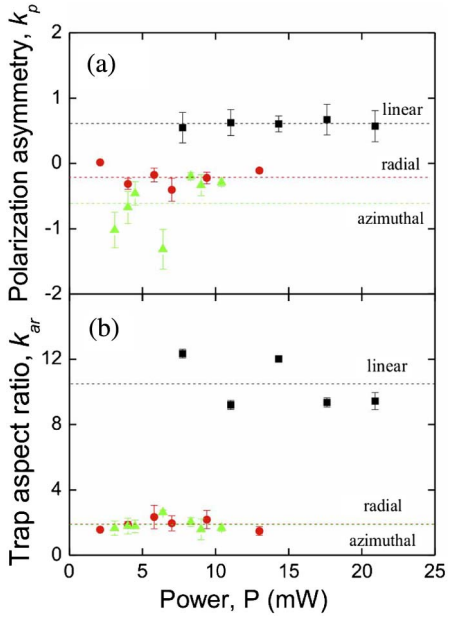

Fig. 3. (Color online) Polarization asymmetry k_p and trap aspect ratio k_{ar} as a function of power under linear (squares), radial (circles), and azimuthal (triangles) polarization. Dashed lines are the average values for each data-set.

The trap aspect ratios [Fig. 3(b)] show the beneficial effect of radial and azimuthal polarization on the axial trapping efficiency, yielding a more isotropic trap with respect to linear polarization.

In conclusion, we have demonstrated optical trapping of nanotubes under radial and azimuthal polarization. We measured the spring constants and geometry of the optical trap, and showed that the trapping potential for 1D nanostructures can be shaped with the use of CVBs. An improvement of axial together with a reduction of transverse trapping efficiency was verified. This is important when using linear nanostructures as probes in photonic force microscopy, where a high axial stiffness will increase the dynamic range, and low axial stiffness can increase resolution for very low (femto-Newton scale) forces.

We acknowledge funding from the Royal Society, the Engineering and Physical Science Research Council (EPSRC), the Newton Trust, and the European Research Council (Grant NANOPOTS: Nanotube Based Polymer Optoelectronics).

References

1. A. Ashkin, J. M. Dziedzic, J. E. Bjorkholm, and S. Chu, Opt. Lett. **11**, 288 (1986).
2. A. Ashkin, *Optical Trapping and Manipulation of Neutral Particles Using Lasers* (World Scientific, 2006).
3. Focus Issue, Nat. Photon. **5**, 315 (2011).
4. K. Dholakia, P. Reece, and M. Gu, Chem. Soc. Rev. **37**, 42 (2008).
5. K. Svoboda and S. M. Block, Opt. Lett. **19**, 930 (1994).
6. E. Messina, E. Cavallaro, A. Cacciola, M. A. Iatì, P. G. Gucciardi, F. Borghese, P. Denti, R. Saija, G. Compagnini, M. Meneghetti, V. Amendola, and O. M. Maragò, ACS Nano **5**, 905 (2011).
7. O. M. Maragò, P. H. Jones, F. Bonaccorso, V. Scardaci, P. G. Gucciardi, A. G. Rohzin, and A. C. Ferrari, Nano Lett. **8**, 3211 (2008).
8. O. M. Maragò, F. Bonaccorso, R. Saija, G. Privitera, P. G. Gucciardi, M. A. Iatì, G. Calogero, P. H. Jones, F. Borghese, P. Denti, V. Nicolosi, and A. C. Ferrari, ACS Nano **4**, 7515 (2010).
9. Y. Nakayama, P. J. Pauzauskie, A. Radenovic, R. M. Onorato, R. J. Saykally, J. Liphardt, and P. Yang, Nature **447**, 1098 (2007).
10. F. Borghese, P. Denti, R. Saija, M. A. Iatì, and O. M. Maragò, Phys. Rev. Lett. **100**, 163903 (2008).
11. A. Irrera, P. Artoni, R. Saija, P. G. Gucciardi, M. A. Iatì, F. Borghese, P. Denti, F. Iacona, F. Priolo, and O. M. Maragò, Nano Lett. **11**, 4879 (2011).
12. D. M. Carberry, S. H. Simpson, J. A. Grieve, Y. Wang, H. Schafer, M. Steinhart, R. Bowman, G. M. Gibson, M. J. Padgett, S. Hanna, and M. J. Miles, Nanotech. **21**, 175501 (2010).
13. P. H. Jones, F. Palmisano, F. Bonaccorso, P. G. Gucciardi, G. Calogero, A. C. Ferrari, and O. M. Maragò, ACS Nano **3**, 3077 (2009).
14. C. Maurer, A. Jesacher, S. Furhapter, S. Bernet, and M. Ritsch-Marte, New J. Phys. **9**, 78 (2007).
15. Q. Zhan, Adv. Opt. Photon. **1**, 1 (2009).
16. J. J. Saenz, Nat. Photon. **5**, 514 (2011).
17. J. Chen, J. Ng, Z. Lin, and C. T. Chan, Nat. Photon. **5**, 531 (2011).
18. K. S. Youngworth and T. G. Brown, Opt. Express **7**, 77 (2000).
19. Q. Zhan, J. Opt. A **5**, 229 (2003).
20. Q. Zhan, Opt. Express **12**, 3377 (2004).
21. F. Peng, B. Yao, S. Yan, W. Zhao, and M. Lei, J. Opt. Soc. Am. B **26**, 2242 (2009).
22. H. Kawauchi, K. Yonezawa, Y. Kozawa, and S. Sato, Opt. Lett. **32**, 1839 (2007).
23. T. Nieminen, N. R. Heckenberg, and H. Rubinsztein-Dunlop, Opt. Lett. **33**, 122 (2008).
24. M. Rashid, O. M. Maragò, and P. H. Jones, J. Opt. A **11**, 065204 (2009).
25. I. Iglesias and J. J. Saenz, Opt. Express **20**, 2832 (2012).
26. R. Dorn, S. Quabis, and G. Leuchs, Phys. Rev. Lett. **91**, 233901 (2003).
27. M. Michihata, T. Hayashi, and Y. Takaya, Appl. Opt. **48**, 6143 (2009).
28. P. H. Jones, M. Rashid, M. Makita, and O. M. Maragò, Opt. Lett. **34**, 2560 (2009).
29. Y. Kozawa and S. Sato, Opt. Express **18**, 10828 (2010).
30. B. J. Roxworthy and K. C. Toussaint, New J. Phys. **12**, 073012 (2010).
31. M. G. Donato, M. A. Monaca, G. Faggio, L. De Stefano, P. H. Jones, P. G. Gucciardi, and O. M. Maragò, Nanotech. **22**, 505704 (2011).
32. F. Bonaccorso, T. Hasan, P. H. Tan, C. Sciascia, G. Privitera, G. Di Marco, P. G. Gucciardi, and A. C. Ferrari, J. Phys. Chem. C **114**, 17267 (2010).